Peptides in motion

Poloni, Claudia

Chapter 6

Photoswitchable zinc finger domain

The use of an azobenzene photoswitch to control the binding of zinc finger Sp1-f3 to DNA is described. The light-responsive unit was inserted in the turn region of the zinc finger domain. The photoisomerization is shown to both influence the binding of the zinc ion and disturb the secondary structure of the peptide. These differences are utilized to achieve photochemical control over the binding of Sp1-f3 to DNA.

6.1 Introduction

Light has been used to control the secondary structure of peptides and to influence the function of larger biomolecules.[1] The main advantages of using light as an external stimulus to control biological processes are the bio-orthogonality, non-invasiveness and lack of toxicity,[1,2] although UV light might be harmful.[3] For controlling biological functions with light, photoswitchable molecules, such as stilbenes,[4] spiropyrans[5] and diarylethenes[6] have been inserted in peptides, proteins and enzymes. In recent years, azobenzenes emerged as a class of photoswitches most widely used to achieve controlled interference with many different biological systems.[1,7]

The control over the formation of secondary structure in peptides was achieved mainly for secondary structural elements, including α-helix,[8] e.g. in basic leucine zipper domains[9] and collagen,[10] and both β-turn and β-strands in β-hairpin structures.[11] Two different approaches were taken for the photomodulation of the secondary structure: the photoswitchable molecules were used as cross-linkers between two side chains or they were inserted into the backbone of the peptide. The first approach has been used mainly to control the formation of α-helix structures.[8] The second approach has been used to interfere with β-turn structures: the azobenzene unit was inserted into the turn region of the peptide.[11]

In this study, we describe a novel approach towards the photochemical control of peptidic structural elements that need ion coordination to adopt the secondary structure. The chosen target was the zinc finger domain, which binds to the major groove of DNA.[12] This element constitutes two β-strands and an α-helix and its secondary structure is stabilized by the coordination of a zinc ion (Zn^{2+}).[13] The α-helix acts as a DNA-binding region.[12] In general, zinc fingers are part of transcription factors that play an important role in gene expression and they are also used in gene therapy.[12] The photocontrol of the binding of these domains to DNA might provide a powerful tool to control externally the expression of a particular gene, which would bring new possibilities in therapy and research.

The control of DNA-binding using a zinc-finger-bearing protein in combination with a light-sensitive molecule has been reported previously by the groups of Deiters[14] and Okamoto.[15] The system described by Deiters and co-workers relies on the concept of caging the biological activity with a photolabile group. The photocontrol does not directly affects the zinc finger domain, but a nuclease domain attached to it, which permits the phototriggering of gene editing *via* double strand break.[14] The design relies on the introduction of a photocaged Tyr residue into the active site of the nuclease Fok1.[14] The zinc finger nuclease (ZFN) was expressed in its photocaged, inactive form, and the irradiation-induced uncaging restored the activity of ZFN and resulted in double strand cut.[14]

Okamoto[15] reported another example on zinc finger peptide, modified with an azobenzene. Here, the switch was introduced at *N*-terminus, close to the α-helix responsible for the DNA binding (Figure 1a), where it can interfere with the DNA binding in a photocontrolled manner. The photoresponsive unit does not influence the secondary structure of the zinc-finger domain, but interferes with the site of DNA-interaction, thus affecting the binding to DNA.[15]

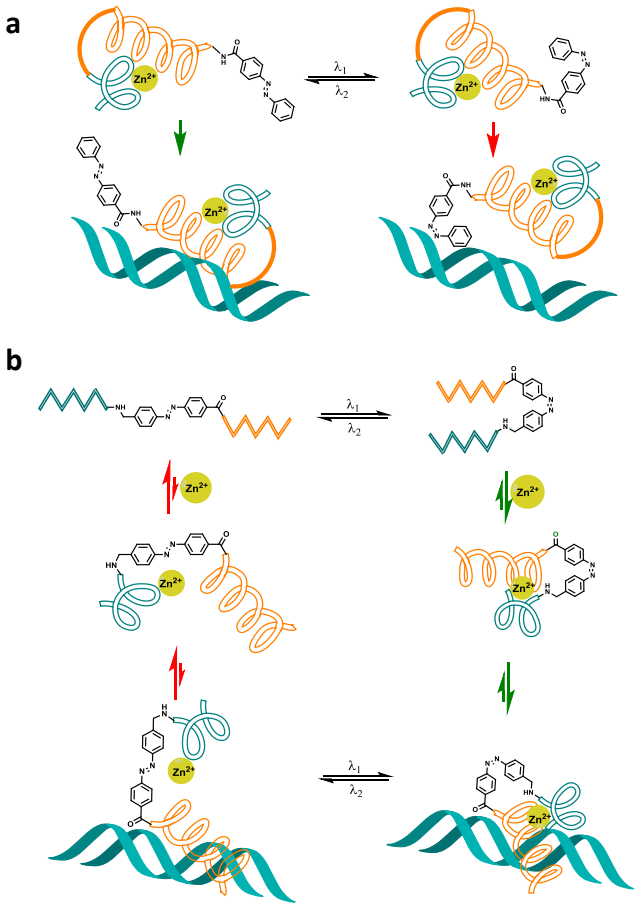

Figure 1: Approaches to photoswitchable zinc-finger domains. a) Photoswitchable zinc finger in which the azobenzene does not interfere with the secondary structure but with DNA-binding only, as described by Okamoto and co-workers.[15] b) Photoswitchable zinc finger in which the azobenzene interferes with the secondary structure and therefore with the DNA-binding (this work).

Here we describe our effort towards a system in which the photoswitchable unit interferes with the Zn^{2+}-mediated formation of the secondary structure and/or induces distortion of the zinc-finger, thereby influencing the binding of the zinc finger to DNA. This design relies on the introduction of an azobenzene switch, (4-

aminomethyl)phenylazobenzoic acid (AMPB) (Figure 2), introduced by Chmielewski *et al.*,[16] in the turn region of third zinc fingers of the mammalian factor Sp1[17] (Figure 2), in expectation that this modification would influence the binding of the zinc ion and, therefore, the secondary structure of the zinc finger domain (Figure 1b), leading to a general approach to photocontrolled zinc fingers. We envisioned that both isomers could bind zinc ions, albeit with different affinities, and the photoswitch would thus influence the secondary structure that would translate into photocontrolled binding to DNA (Figure 1b).

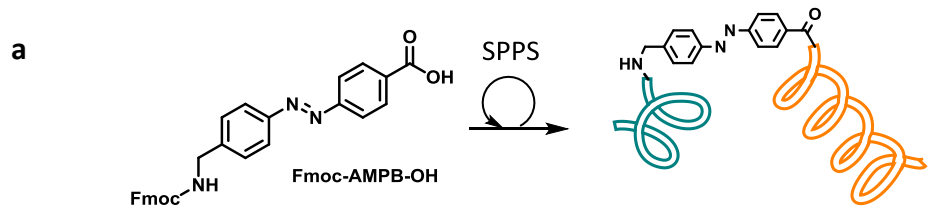

Figure 2: a) Fmoc-AMPB-OH,[16,18] building block for SPPS, used for the synthesis of AMPB-Sp1-f3. b) Sequence of AMPB-Sp1-f3 and the natural sequence Sp1-f3.[17] The amino acids in yellow are the ones involved in the binding of zinc ion.

6.2 Results and Discussion

The preparation of the photoswitchable Sp1-f3, dubbed AMPB-Sp1-f3, was achieved using solid phase peptide synthesis (SPPS) (Figure 2). The azobenzene building block (Figure 2a), used for SPPS, was reported previously.[16,18] In line with published data,[19] we observed that the use of silanes, which are added as cation scavengers in traditional SPPS cleavage/deprotection cocktails, resulted in the reduction of the diazo moiety of the photoswitch;[19] therefore, their use was avoided. Pure peptide was obtained by preparative HPLC and its identity was confirmed by MALDI-TOF mass analysis (Figure 3a,b). The natural Sp1-f3 (Figure 2b) was synthesized as well, to serve as a reference compound (Figure 3c,d).

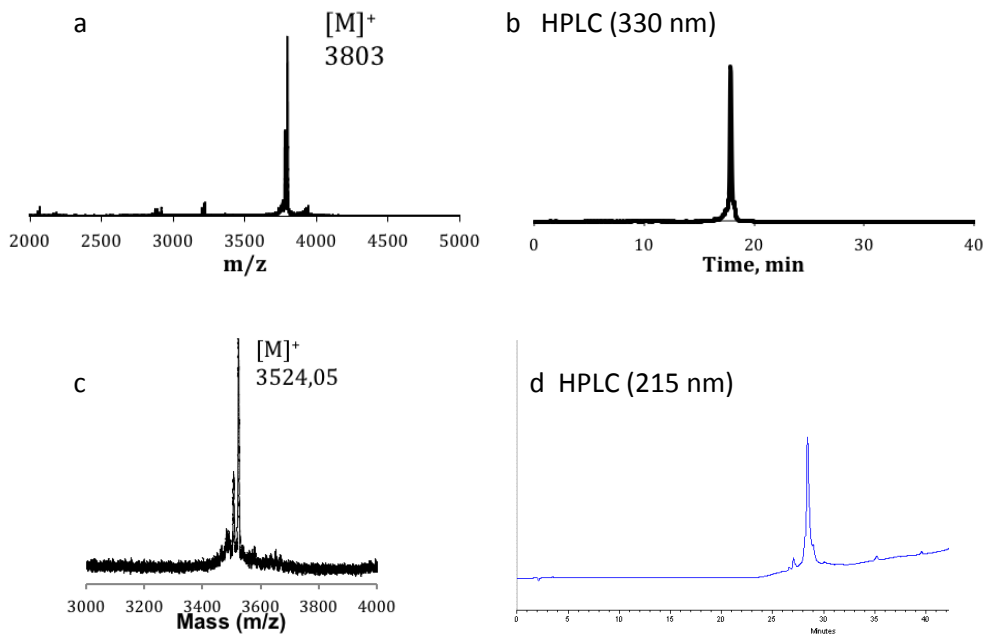

Figure 3: Analysis for AMPB-Sp1-f3 and Sp1-f3**.** a) MALDI-TOF spectrum of AMPB-Sp1-f3**.** b) HPLC trace of AMPB-Sp1-f3**.** RP-HPLC method: 3 min at ratio of eluents A:B 5/95 and then linear gradient of 1.54% of eluent A per min at a flow rate of 0.5 mLmin^{-1}. The eluents A and B are 0.1 % TFA acetonitrile and 0.1 % $_{aq}$TFA, respectively (XTerra C18 3.0x150 mm column, Waters). c) MALDI-TOF spectrum of Sp1-f3**.** d) HPLC trace of Sp1-f3 (detection at λ = 215 nm)**.** RP-HPLC method: 10 min at ratio of eluents A:B 5/95 and then linear gradient of 3% of eluent A per min at a flow rate of 0.5 mLmin^{-1}. The eluents A and B are 0.1 % TFA acetonitrile and 0.1 % $_{aq}$TFA, respectively (XTerra C18 3.0x150 mm column, Waters).

The photoswitching behaviour of AMPB-Sp1-f3 in DMSO/MeOH was analysed by UV-vis spectroscopy and HPLC. The UV-vis spectrum (Figure 4a) of the *trans* isomer is characterized by the band at λ = 330 nm. Upon irradiation at λ = 365 nm, this band decreases and a new low intensity one, characteristic for the *cis* form, appears at λ = 450 nm (Figure 4a). By exposition of the *cis* isomer to white light, the equilibrium is shifted back towards the stable *trans* form (Figure 4a, WL). AMPB-Sp1-f3 is stable at least over three switching cycles in DMSO/MeOH (Figure 4b). The photostationary state (PSS) in aqueous buffer was determined by HPLC analysis to be >45%[20] *cis* (Figure 4d). The photochemical properties of the azobenzene are in agreement with other reported systems,[8,9] with relatively high photostationary state and reversible photoisomerization.

The half-life for the thermally less-stable *cis* isomer of AMPB-Sp1-f3 was determined by following the recovery of the absorbance at λ = 330 nm of the photoisomerized sample in the dark (Figure 4c). The experiment was conducted both

in the presence and absence of zinc ions, to verify if the zinc binding influences the half-life of the azobenzene-peptide. By fitting the experimental data with single exponential decay, the half-life was calculated to be 36 h in presence of zinc ion and 14 h in absence of zinc ion (Figure 4c). This effect indicates, interestingly, that the zinc coordination influences the stability of the *cis* isomer. Since the coordination of zinc is responsible for the formation of secondary structure,[12] we attribute this increased stability of the *cis* isomer to the folding of the peptide.

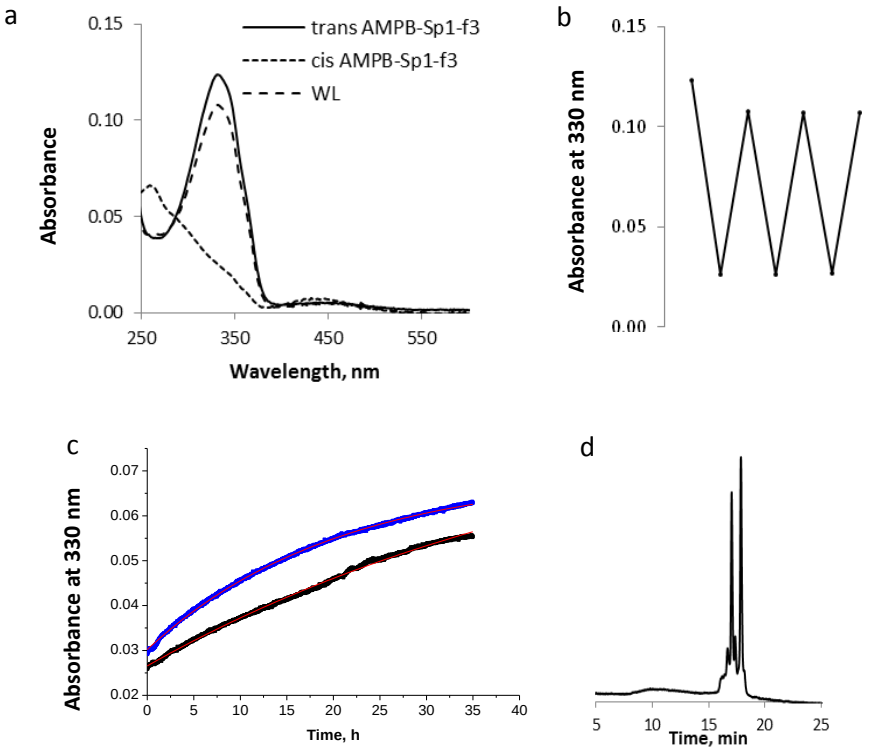

Figure 4: Photoswitching behaviour of AMPB-Sp1-f3. a) UV-vis spectra of *trans*- and *cis*-AMPB-Sp1-f3 (0.084 mM in DMSO/MeOH (1:9)). b) Switching cycle of AMPB-Sp1-f3 (0.084 mM in DMSO/MeOH (1:9)). c) Determination of half-life of *cis*-AMPB-Sp1-f3 (0.055 mM in 10 mM TRIS buffer, 50 mM $_{aq.}$NaCl, pH 7.5) by UV-vis spectroscopy, in presence (black line) or absence (blue line) of zinc ion ($ZnCl_2$, 1 eq. respect to *cis*-AMPB-Sp1-f3), at rt in the dark. d) HPLC trace of AMPB-Sp1-f3 at isosbestic point (λ = 386 nm) after irradiation for 3 min at λ = 365 nm in water. RP-HPLC method: 3 min at ratio of eluents A:B 5/95 and then linear gradient of 1.54% of eluent A per min at a flow rate of 0.5 mLmin^{-1}. The eluents A and B are 0.1 % TFA acetonitrile and 0.1 % $_{aq}$TFA, respectively (XTerra C18 3.0x150 mm column, Waters).

The formation of secondary structure of Sp1-f3 was confirmed by CD spectroscopy.[21] The peptide is in random coil conformation in the absence of zinc, which is characterized by the negative CD signal at $\lambda \approx 200$ nm.[15,21] The appearance of

two negative CD signals (at λ = 205 nm and λ = 228 nm), indicative of the formation of the secondary structure of the zinc finger, is observed upon addition of zinc ions.[15,21] Here, CD spectroscopy was used to verify whether the *trans*- and *cis*-AMPB-Sp1-f3 adopt the secondary structure characteristic of a zinc finger upon addition of zinc ions (Figure 5). Furthermore, the CD signal change upon addition of aliquots of Zn^{2+} were used to provide information about the affinity to zinc (Figure 5).

The model, unmodified Sp1-f3, was used for comparison; for this peptide, the characteristic spectrum for the zinc finger is observed upon addition of Zn^{2+} (Figure 5a). [15,21] Two negative CD signals are observed at λ = 205 nm and λ = 226 nm (Figure 5a), consistent with reported data.[21] From CD analysis of the AMPB-Sp1-f3 (Figure 5b), it is clear that neither the *trans* nor *cis* isomers are able to adopt the secondary structure in absence of zinc ion: a negative CD signal at $\lambda \approx$ 200 nm is present, which is characteristic of random coil. Next 1 eq. of Zn^{2+} was added to the *cis*-AMPB-Sp1-f3 and the CD signal characteristic for the formation of secondary structure manifested at λ = 205 nm (Figure 5b). The solution of Zn^{2+}-bound *cis*-AMPB-Sp1-f3 was then irradiated with white light. This operation provokes, at least partially, reisomerisation of the photoswitch to the *trans* form, as confirmed by UV-vis spectroscopy (see insert, Figure 5b). Nevertheless, we observed almost no change in the CD spectrum (Figure 5b), which means that both *trans*- and *cis*-AMPB-Sp1-f3 can coordinate zinc and form the secondary structure of the zinc finger.

The affinity of the two isomers of AMPB-Sp1-f3 to zinc was studied in more detail using CD spectroscopy,[21] focusing on the band at λ = 205 nm (Figure 5c,d). The increase of the CD signal at λ = 205 nm with the addition of Zn^{2+} gives as an indication of the binding constant of zinc to the peptide. It was found that *trans*-AMPB-Sp1-f3 has a K_d =1.4 eq (Figure 5c) and *cis*-AMPB-Sp1-f3 has a K_d = 0.7 eq (Figure 5d), where K_d is defined as the number of Zn^{2+} equivalents that leads to 50% folding of AMPB-Sp1-f3 into a secondary structure. The fact that *cis*-AMPB-Sp1-f3 is a very strong zinc-binder, might be explain by the spatial arrangement that the *cis*-form provokes in the zinc finger domain. Probably this isomer brings together the amino acids, His and Cys, involved in the zinc-binding favoring the binding to the zinc ion (Figure 1b).

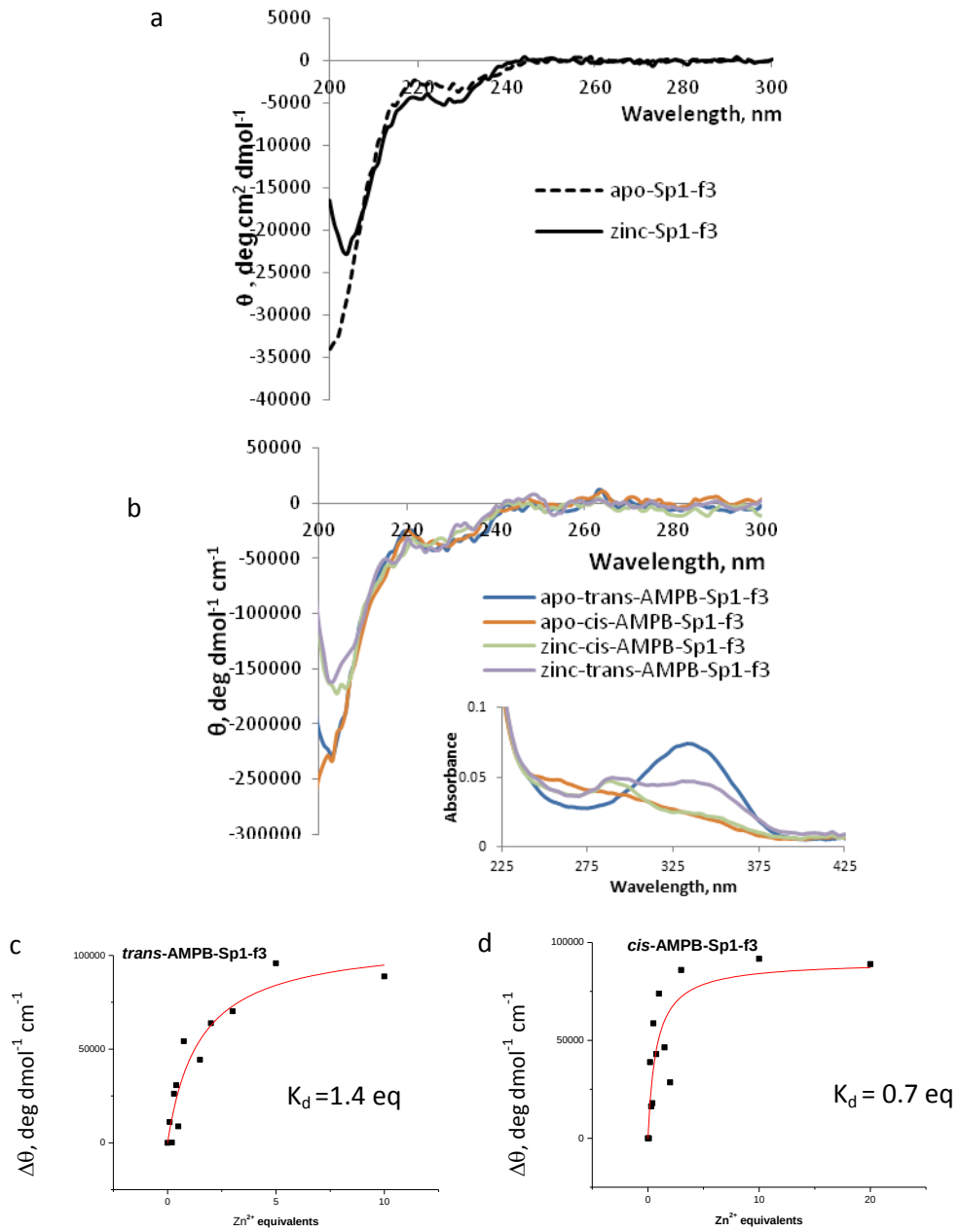

Figure 5: Secondary structure of Sp1-f3 and AMPB-Sp1-f3 analysed by CD spectroscopy. a) CD spectra of Sp1-f3 (0.055 mM in 10 mM TRIS, 50 mM NaCl, pH 7.5) in the presence and the absence of Zn^{2+}. b) CD spectra of *cis*- and *trans*-AMPB-Sp1-f3 (0.055 mM in 10 mM TRIS, 50 mM NaCl, pH 7.5) in the presence or absence of Zn^{2+}. c) Increase in CD signal at λ = 205 nm for *trans*-AMPB-Sp1-f3 (0.055 mM in 10 mM TRIS, 50 mM NaCl, pH 7.5) upon addition of aliquots of Zn^{2+}. d) Increase in CD signal at λ = 205 nm for *cis* AMPB-Sp1-f3 (0.055 mM in 10 mM TRIS, 50 mM NaCl, pH 7.5), upon addition of aliquots of Zn^{2+}.

The binding of AMPB-Sp1-f3 to DNA was studied using a fluorescence displacement assay.[22,23] This assay is used to define the DNA-binding affinity of molecules compared to a known intercalator, e.g. ethidium bromide (EB). In general, model double-stranded DNA is incubated with EB and the studied peptide or molecule is titrated into the DNA solution. Ethidium bromide is highly fluorescent when it intercalates into DNA, and shows low fluorescence in the unbound form. The addition of peptide displaces EB molecules, which is accompanied by the decrease in fluorescence. This assay has been successfully used for molecules that bind to the minor groove[23] and major groove of DNA.[22]

The fluorescence displacement assay was executed for natural zinc finger, Sp1-f3, and the two photoisomers of AMPB-Sp1-f3, using double-stranded DNA, GC-box (d-ATA TTA TGG GGC GGG GCC AAT ATA) intercalated with EB. The assay was performed in triplicate and the data were analysed by exponential fitting,[22,23] from which IC_{50} values were calculated (Figure 6). The IC_{50} represents the ratio of EB and peptide concentrations that is necessary to displace half of the EB molecules from DNA. For Sp1-f3, the IC_{50} is 0.4 ± 0.1 (Figure 6a), in accordance with values reported in literature for a major-groove-binder.[22] As a control, the assay was repeated in absence of zinc to provide an additional confirmation that zinc is necessary for the binding. We observed no fluorescence decrease, indicative of no EB displacement, using up to 100 eq. of apo-Zinc finger (Figure 6b). We conclude that the peptide Sp1-f3 without zinc ion doesn't bind DNA, most probably due to the lack of secondary structure formation (Figure 5a).

The assay for AMPB-Sp1-f3 revealed that both photoisomers can bind DNA: in presence of Zn^{2+}, *trans*-AMPB-Sp1-f3 has $IC_{50} = 0.7\pm0.1$ (Figure 6c) and for *cis*-AMPB-Sp1-f3, the IC_{50} is 0.36 ± 0.07 (Figure 6d). The IC_{50} value for *cis*-AMPB-Sp1-f3 is similar to the natural Sp1-f3, while, remarkably, the IC_{50} value for *trans*-AMPB-Sp1-f3 is higher than the IC_{50} value for *cis* one, indicating that *trans*-AMPB-Sp1-f3 is a stronger DNA-binder.

CD analysis reveals that the secondary structure is formed with both the photoisomers, although the affinity for Zn^{2+} ion is different between the *trans*- and *cis*-form, with K_d =1.4 eq for *trans*-AMPB-Sp1-f3 and K_d = 0.7 eq for *cis*-AMPB-Sp1-f3. Even if both the photoisomers promote the formation of the zinc finger domain, EB displacement assay shows that there is a distinctive difference in binding to DNA. We propose that the structure of the zinc finger incorporated the *cis* isomer is distorted and therefore a weaker binding to DNA is observed with respect the *trans* isomer.

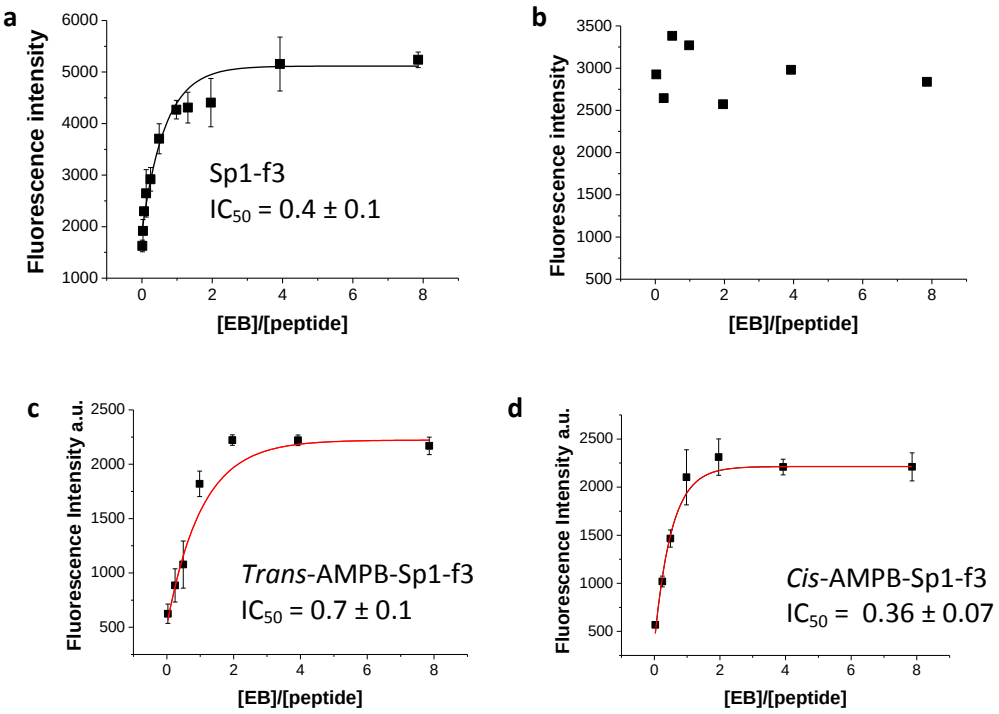

Figure 6: Fluorescence EB displacement assay (8.8 µM-bp GC-box (d-ATA TTA TGG GGC GGG GCC AAT ATA), 0.22 mM solution of ethidium bromide in 10 mM TRIS buffer, NaCl 50 mM, pH 7.5; aliquots of peptide ($2.8 \cdot 10^{-4}$ M in in 10 mM TRIS buffer, NaCl 50 mM, pH7.5) and Zn^{2+} were added at 25 °C). a) EB displacement assay for Sp1-f3 in the presence of zinc ion. b) EB displacement assay for Sp1-f3 in the absence of zinc ion. c) EB displacement assay for *trans*-AMPB-Sp1-f3 in the presence of 1 equivalent of zinc ion with respect to the peptide. d) EB displacement assay for *cis*-AMPB-Sp1-f3 in presence of 1 equivalent of zinc ion with respect to the peptide.

Interestingly, *trans*-AMPB-Sp1-f3 is a weaker binder of Zn^{2+} and a stronger DNA-binder than the *cis*-AMPB-Sp1-f3 and the natural Sp1-f3. It might be that the spatial arrangement, induced by the *trans*-azobenzene, stabilizes even further the α-helix, which is responsible for DNA binding. The *trans* isomer binds two times stronger to DNA than the *cis* form; this effect is similar to the one reported for the modified zinc finger of Okamoto.[15] Despite of this similar behavior, the two approaches (Figure 1a for Okamoto and Figure 1b for our system) are conceptually different: the difference in binding in our system is due to the distortion of the structure of the zinc finger that the azobenzene induces and not to the interference with the DNA-binding region of the zinc finger as reported for the system of Okamoto.[15]

6.3 Conclusions

We presented here a photoswitchable zinc finger, AMPB-Sp1-f3, which incorporates an azobenzene unit in the turn region. The photochemical isomerization studies of this system showed that the azobenzene has a photostationary state of at least 45% *cis* isomer and shows reversible photoisomerization. Furthermore, the half-life of the *cis* isomer depends on the presence of zinc ions.

Both isomers bind zinc ion and form the secondary structure of zinc finger, as shown by CD, therefore both *trans* and *cis* forms can bind to DNA. Interestingly, *cis*-AMPB-Sp1-f3 is a stronger zinc-binder, but a weaker DNA-binder than *trans*-AMPB-Sp1-f3. This might be explained by a better stabilization of the α-helix in the *trans*-isomer.

In summary, we presented here an alternative approach to obtain control of the secondary structure of the zinc finger and, therefore, of the binding to DNA of the zinc finger domain, which potentially is more generally applicable to control zinc finger domains as it does not interfere with specific α-helix-DNA interactions.

6.4 Acknowledgments

We thank Ms. Malgorzata Marta Hiacynta Murawska for her contributions to the experimental work.

6.5 Experimental Section

6.5.1 Synthesis

All chemicals for synthesis were obtained from commercial sources and used as received unless stated otherwise. Solvents were reagent grade. DNA was purchased from Sigma-Aldrich. Thin-layer chromatography (TLC) was performed using commercial Kieselgel 60, F254 silica gel plates, and components were visualized with $KMnO_4$ or phosphomolybdic acid reagent. Flash chromatography was performed on silica gel (Silicycle Siliaflash P60, 40-63 m, 230-400 mesh). Drying of solutions was performed with $MgSO_4$ and solvents were removed with a rotary evaporator. Chemical shifts for NMR measurements were determined relative to the residual solvent peaks ($CHCl_3$, δ = 7.26 ppm for hydrogen atoms, δ = 77.0 for carbon atoms). The following abbreviations are used to indicate signal multiplicity: s, singlet; d, doublet; t, triplet; q, quartet; m, multiplet; br s, broad signal. HRMS (ESI) spectra were obtained on a Thermo scientific LTQ Orbitrap XL. MALDI spectra were obtained on a MALDI/TOFTOF 4800 by AB Sciex; the analysis was done in positive mode using the matrix *alpha*-cyano-hydroxycinnamic acid. Solid phase peptide synthesizer CEM Liberty, with CEM Discover microwaves was used for solid phase peptide synthesis. Optical rotations were measured on a Schmidt + Haensch polarimeter (Polartronic MH8) with a 10 cm cell (c given in g/100 mL) at 20 °C. Melting points were recorded using a Buchi melting point B-545 apparatus. UV/Vis absorption spectra were recorded on an Agilent 8453 UV-Visible Spectrophotometer using Uvasol-grade solvents. CD spectra were recorded on JASCO J815. Irradiation experiments were performed with a spectroline ENB-280C/FE UV lamp (312 nm). RP-HPLC was carried out with Shimadzu equipment using a linear gradient of eluent A at a flow rate of 0.5mLmin^{-1}. The eluents A and B are 0.1 % TFA acetonitrile and 0.1 % $_{aq}$TFA, respectively. For analytical RP-HPLC, a XTerra C18 3.0x150mm column (Waters) was used and for semi-preparative RP-HPLC, a XTerra Prep C18 7.8x150mm column (Waters) was used.

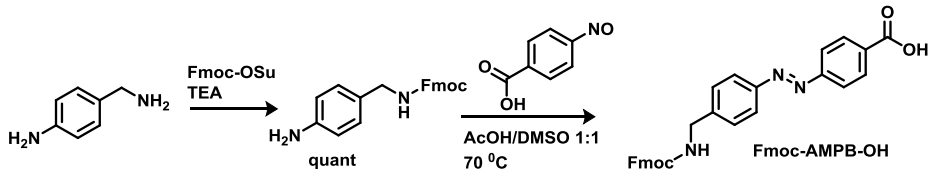

Synthesis of 4-Nitroso-benzoic acid

4-Nitroso-benzoic acid was synthesized according to a literature procedure.[24]

Synthesis of Fmoc-4-aminobenzylamine[16a]

4-Aminobenzylamine (1.25 g, 10.0 mmol) was dissolved in a mixture of 12 mL acetonitrile and 1 mL DMF. Triethylamine (1.55 mL, 11.0 mmol) was added. A solution of Fmoc-OSu (3.70 g, 11.0 mmol in 25 mL of acetonitrile) was added drop-wise over 90 min. The formed precipitate was filtered, washed with water and diethyl ether. The product was obtained in 98% yield (3.37 mg). M. p.: 138-139 °C. ^{1}H-NMR (400 MHz, DMSO-d_6): δ 7.89 (d, *J* = 7.5 Hz, 2H), 7.69 (d, *J* = 7.5

Hz, 2H), 7.65 (m, 1H), 7.41 (t, *J* = 7.3 Hz, 2H), 7.32 (t, *J* = 7.3 Hz, 2H), 6.88 (d, *J* = 7.7 Hz, 2H), 6.49 (d, *J* = 7.7 Hz, 2H), 4.95 (s, 2H), 4.30 (d, *J* = 6.7 Hz, 2H), 4.21 (t, *J* = 6.8 Hz, 1H), 4.00 (d, *J* = 5.8 Hz, 2H). HRMS (ESI+) calc. for $C_{22}H_{21}N_2O_2$ [M+H$^+$]: 345.1598; found: 345.1603.

Synthesis of Fmoc-AMPB-OH[18]

4-Nitroso-benzoic acid (69 mg, 0.46 mmol) was dissolved in 4 mL acetic acid/DMSO (1:1) and Fmoc-4-aminobenzylamine (150 mg, 0.46 mmol) was added. The reaction mixture was stirred overnight at 40 °C. Ethyl acetate was added and the organic solution was washed 5 times with brine. The organic phase was dried ($MgSO_4$), filtered and the solvent was evaporated under vacuum. The product was purified by column chromatography (Eluent: 2% Methanol in DCM). The product was obtained in 33% yield (71 mg). M. p.: 240-242 °C. ^{1}H NMR (400 MHz, DMSO-d_6) δ 13.27 (s, 1H), 8.15 (d, *J* = 8.0 Hz, 2H), 7.96 (d, *J* = 8.0 Hz, 2H), 7.90 (m, 4H), 7.71 (d, *J* = 7.7 Hz, 2H), 7.51–7.39 (m**,** 4H), 7.34 (t, *J* = 7.5 Hz, 2H), 4.39 (d, *J* = 6.7 Hz, 2H), 4.29 (d, *J* = 6.1 Hz, 2H), 4.25 (t, *J* = 6.9 Hz, 1H). HRMS (ESI+) calc. for $C_{29}H_{24}N_3O_4$ [M+H$^+$]: 478.1761; found: 478.1760.

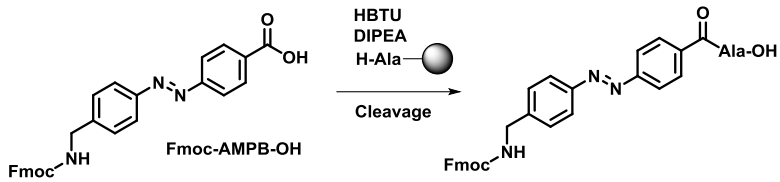

Synthesis of Fmoc-AMPB-Ala-OH

The synthesis was performed using H-Ala-2-Cl-Trt resin (22 mg, 0.72 mmol/g). The resin was swollen in DCM and washed with DMF. A solution of Fmoc-AMPB-OH (15 mg, 0,031 mmol), HBTU (11.7 mg, 0.031 mmol) and DIPEA (11 uL, 0.062 mmol) in DMF was added to the resin. The mixture was shaken for 3 h at rt. The resin was washed with DMF, DCM and diethyl ether. Cleavage from the resin was performed at rt for 75 min with TFA:water (95:5) under a nitrogen atmosphere. The resin was filtered off and the product was obtained by precipitation with diethyl ether. The product was obtained in 76% yield (6.5 mg). M. p.: 255-257 °C. $[\alpha]_D^{20}$ = -7.8 (c = 1.00, DMSO). ^{1}H NMR (400 MHz, DMSO-d_6) δ 12.60 (s, 1H), 8.87 (d, *J* = 7.1 Hz, 1H), 8.10 (d, *J* = 8.4 Hz, 2H), 7.96 (d, *J* = 8.5 Hz, 4H), 7.90 (d, *J* = 7.7 Hz, 4H), 7.72 (d, *J* = 7.3 Hz, 2H), 7.43 (t, *J* = 8.9 Hz, 2H), 7.34 (t, *J* = 7.4 Hz, 2H), 7.25 (s, 1H), 4.46 (s, 1H), 4.40 (d, *J* = 6.7 Hz, 2H), 4.32-4.20 (m, 3H), 1.43 (d, *J* = 7.4 Hz, 3H). ^{13}C NMR (400 MHz, DMSO-d_6) δ 174.1, 165.3, 156.4, 153.4, 150.9, 144.1, 143.8, 140.8, 135.9, 128.8, 127.9, 127.6, 127.0, 125.1, 122.8, 122.3, 120.12, 65.3, 48.3, 46.8, 43.5, 16.8. HRMS (ESI+) calc. for $C_{32}H_{29}N_4O_5$ [M+H$^+$]: 549.2132; found: 549.2127.

Synthesis of AMPB-Sp1-f3 (Ac-KKFACPECPKRFM - AMPB - RSDHLSKHIKTHQNKK-NH$_2$)

AMPB-Sp1-f3 was synthesized on a 0.1 mmol scale by standard protocol of Fmoc chemistry SPPS (Solid Phase Peptide Synthesis) with the peptide synthesizer. Sieber resin was used (0.69 mmol/g). Fmoc-Ala-OH, Fmoc Phe-OH, Fmoc-Cys(Trt) Fmoc-Lys(Trt)-OH, Fmoc-Pro-OH, Fmoc-Glu(O-2-PhiPr)-OH, Foc Arg(Pbf)-OH, Foc-Met-OH, Fmoc-Ser(Trt)-OH, Fmoc-Asp(O-2-PhiPr)-OH,

Fmoc-His(Trt)-OH, Fmoc-Leu-OH, Fmoc-Ile-OH, Fmoc-Thr(Trt)-OH, Fmoc-Gln(Trt)-OH, Fmoc-Asn(Trt)-OH were used. The coupling steps were performed with 5 eq Fmoc-protected amino acid, 5 eq HBTU and 10 eq DIPEA (2 x 45 min). The Fmoc-deprotection step was performed with 20% piperidine in DMF (1 x 30 min). The acetylation step was performed with 10 eq. Ac_2O, 0.1 eq. HOBt and 10 eq. DIPEA. Cleavage from the resin was performed at rt for 75 min with TFA:water (95:5) under a nitrogen atmosphere. The crude peptide was purified by RP-HPLC on C18 semi-preparative column. Purity: 86%. R.t.: 17.8 min. The MALDI-TOF spectrum and the HPLC trace are reported in Figure 3a, b.

Synthesis of Sp1-f3

Sp1-f3 was synthesized on a 0.1 mmol scale by the standard protocol of Fmoc chemistry SPPS (Solid Phase Peptide Synthesis) with the peptide synthesizer. Sieber resin was used (0.69 mmol/g). Fmoc-Ala-OH, Fmoc Phe-OH, Fmoc-Cys(Trt) Fmoc-Lys(Boc)-OH, Fmoc-Pro-OH, Fmoc-Glu(O*t*Bu)-OH, Foc Arg(Pbf)-OH, Foc-Met-OH, Fmoc-Ser(*t*Bu)-OH, Fmoc-Asp(O*t*Bu)-OH, Fmoc-His(Trt)-OH, Fmoc-Leu-OH, Fmoc-Ile-OH, Fmoc-Thr(*t*Bu)-OH, Fmoc-Gln(Trt)-OH, Fmoc-Asn(Trt)-OH were used. The coupling steps were performed with 5 eq Fmoc-protected amino acid, 5 eq HBTU and 10 eq DIPEA (2 x 45 min). The Fmoc-deprotection step was performed with 20% piperidine in DMF (1 x 30 min). The acetylation step was performed with 10 eq. Ac_2O, 0.1 eq. HOBt and 10 eq. DIPEA. Cleavage from the resin was performed at rt for 75 min with TFA/TIS/EDT/H_2O (95:1:2.5:2.5) under a nitrogen atmosphere. The crude peptide was purified by RP-HPLC on C18 semi-preparative column. Purity: 80%. Ret. Time: 28.3 min. The MALDI-TOF spectrum and the HPLC trace are reported in Figure 3c, d.

6.5.2 Spectroscopic studies

Determination of the extinction coefficient, ε, for Fmoc-AMPB-Ala-OH

Solutions of different concentrations of Fmoc-AMPB-Ala-OH were prepared in DMSO/MeOH (1:9): 0.011 mM, 0.022 mM, 0.032 mM, 0.042 mM, 0.061 mM (Figure 7a). The UV-vis absorption spectra were recorded and the extinction coefficient at 330 nm was calculated from the plot of absorbance at 330 nm against the concentration (Figure 7b).

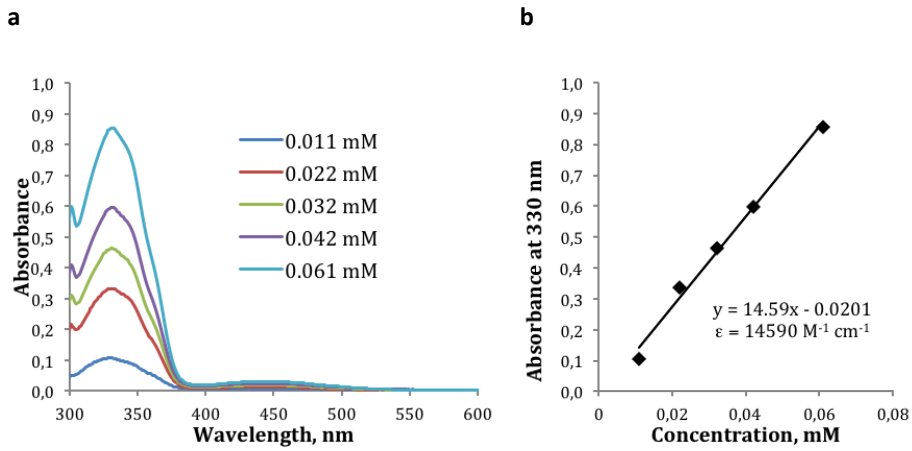

Figure 7: a) UV-vis absorption spectra for solutions of Fmoc-AMPB-Ala-OH in DMSO/MeOH (1:9) at different concentrations. b) Absorbance at λ = 330 nm vs. the concentration of the different samples.

Switching cycle for AMPB-Sp1-f3 by UV-vis spectroscopy

AMPB-Sp1-f3 (DMSO/MeOH (1:9)) was irradiated at λ = 365 nm and subsequently with white light. The changes in absorbance were followed by UV-vis absorption (Figure 4a,b). The concentration was determined to be 0.084 mM, using ε of the standard compound, Fmoc-AMPB-Ala-OH.

AMPB-Sp1-f3 (0.055 mM in 10 mM TRIS, 50 mM NaCl, pH 7.5) was irradiated at λ = 365 nm. The change in absorbance at λ = 330 nm was followed (Figure 8). The half-life was calculated following the increase in absorbance at λ = 330 nm at rt in the dark, in the absence and in the presence of 1 eq $ZnCl_2$ (Figure 4c), by fitting with first exponential decay. The concentration was calculated using ε of the standard compound, Fmoc-AMPB-Ala-OH.

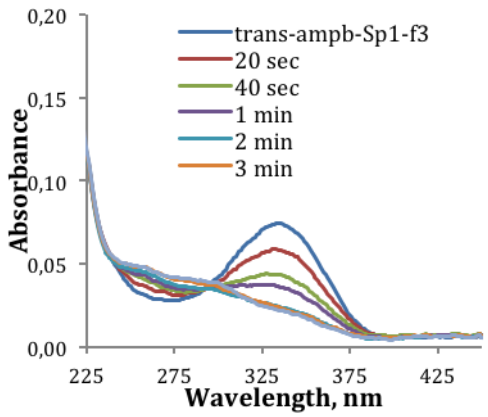

Figure 8: UV-vis spectrum of *trans* AMPB-Sp1-f3 (0.055 mM in aqueous solution containing 10 mM TRIS, 50 mM NaCl at pH 7.5) and UV-vis spectra recorded during irradiation at λ = 365 nm.

Determination of photostationary state of the AMPB-Sp1-f3 by HPLC

AMPB-Sp1-f3 (0.5 mg/mL H_2O) was irradiated with λ = 365 nm light for 3 min and injected in the HPLC. The photostationary state was calculated form the absorption at λ = 386 nm (isosbestic point) (Figure 4d).

CD spectroscopy for Sp1-f3

The CD spectra of Sp1-f3 (0.030 mM in 10 mM TRIS buffer, 50 mM NaCl, pH 7.5) were recorded before and after the addition of 1 µL of a stock solution of $ZnCl_2$ (27 mM in H_2O, 3 eq.) (Figure 5a, Figure 9).

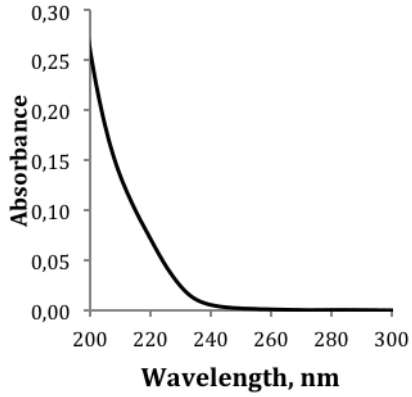

Figure 9: UV-vis spectrum of Sp1-f3 (0.030 mM in aqueous solution containing 10 mM TRIS buffer, 50 mM NaCl at pH 7.5).

CD spectroscopy for AMPB-Sp1-f3: determination of K_d for *trans*-azo-zinc finger and *cis*-azo-zinc finger with Zn^{2+}

Trans AMPB-Sp1-f3 (0.055 mM in 10 mM $_{aq.}$TRIS buffer, 50 mM NaCl, pH 7.5) was irradiated at λ = 365 nm and the change in CD signal was followed (Figure 5b, Figure 10a). The corresponding UV-vis spectra are shown in Figure 5b, inset and Figure 10b. The concentration of *trans*-AMPB-Sp1-f3 was calculated using the extinction coefficient (ε) of the standard compound, Fmoc-AMPB-Ala-OH.

Titration of $ZnCl_2$ into an aqueous solution of *trans*-AMPB-Sp1-f3: Zn^{2+} ($ZnCl_2$, 0.1-10 eq. with respect to *trans*-AMPB-Sp1-f3) was titrated into the solution of *trans*-AMPB-Sp1-f3 and UV-vis spectra and CD spectra were recorded (Figure 5c).

Titration of $ZnCl_2$ into an aqueous solution of *cis* AMPB-Sp1-f3: *trans* AMPB-Sp1-f3 was irradiated at λ = 365 nm to form *cis*-AMPB-Sp1-f3 (Figure 10c). Zn^{2+} ($ZnCl_2$, 0.1-20 eq. with respect to *cis*-AMPB-Sp1-f3) was titrated into the aq. solution of *cis*-AMPB-Sp1-f3 and UV-vis spectra and CD spectra were recorded (Figure 5d). From these data, the titration curves are

obtained and fitted with single exponential decay. The corresponding UV-vis spectra for the CD spectra of Figure 5d (0.1 eq., 1 eq. and 10 eq) are reported in Figure 10d.

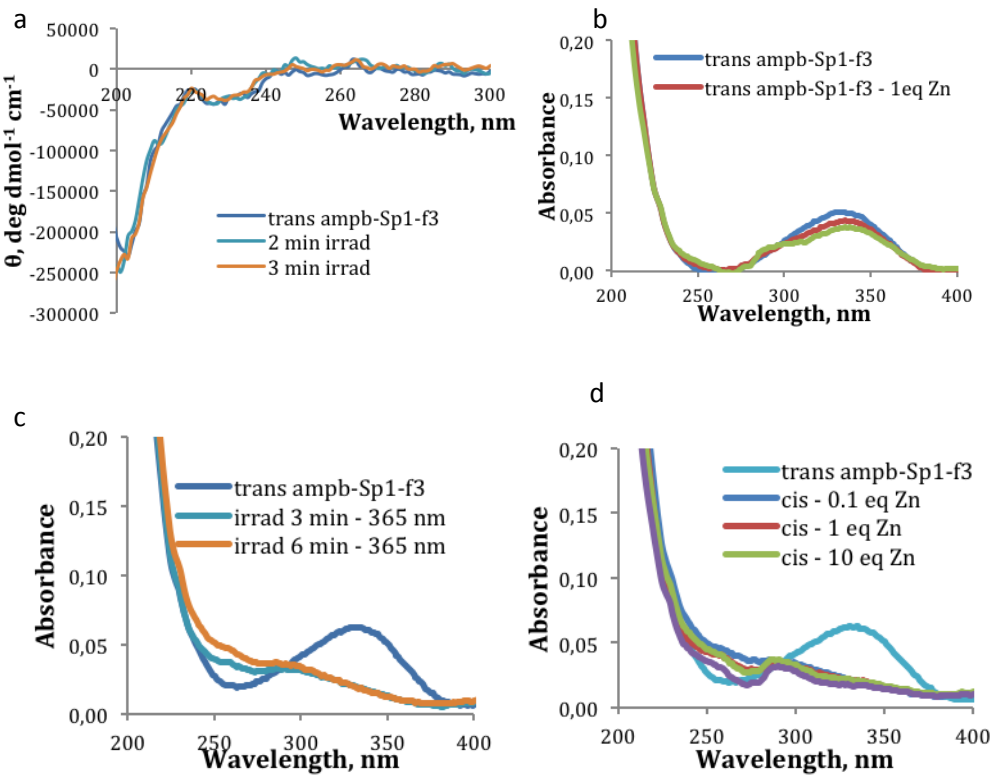

Figure 10: CD and UV-vis analysis of AMPB-Sp1-f3 (0.055 mM in 10 mM $_{aq.}$TRIS buffer, 50 mM NaCl, pH 7.5). a) CD spectra of *trans*-AMPB-Sp1-f3 (0.055 mM in 10 mM $_{aq.}$TRIS buffer, 50 mM NaCl, pH 7.5), before and after irradiation at λ = 365 nm in the absence of Zn^{2+}. b) UV-vis spectra of *trans*-AMPB-Sp1-f3 (0.055 mM in 10 mM $_{aq.}$TRIS buffer, 50 mM NaCl, pH 7.5). in the absence or the presence of Zn^{2+} (1 eq and 10 eq). c) UV-vis spectra of *trans*-AMPB-Sp1-f3 (0.055 mM in 10 mM $_{aq.}$TRIS buffer, 50 mM NaCl, pH 7.5) before and after irradiation at λ = 365 nm in the presence of Zn^{2+}. d) UV-vis spectra of *cis*-AMPB-Sp1-f3 (0.055 mM in 10 mM $_{aq.}$TRIS buffer, 50 mM NaCl, pH 7.5) in the absence or the presence of Zn^{2+} (0.1 eq, 1 eq and 10 eq).

6.5.3 Ethidium Bromide displacement assay

Solution A: 8.8 µM (base pairs) solution of GC-box (d-ATA TTA TGG GGC GGG GCC AAT ATA) in 10mM $_{aq.}$TRIS buffer, NaCl 50 mM, pH7.5. The solution was heated up to 90 °C and cooled down to -5 °C prior to titration experiments, to assure annealing of DNA strands.

Solution B: 0.22 mM solution of ethidium bromide (EB) in water.

Solution A and B were mixed to obtain a 2:1 of ratio base pairs/EB. Aliquots (0-52.2 µL) of peptide ($2.8 \cdot 10^{-4}$ M in in 10 mM $_{aq.}$TRIS buffer, NaCl 50 mM, pH7.5) were added. $ZnCl_2$ solution was added to obtain 1:1 ratio Zn^{2+}/peptide. The wells were filled with buffer to obtain a constant volume. The assay was performed in a black 96-well microtiter plate and fluorescence

was recorded in the plate reader Synergy- H1, Biotek (λ_{ex} = 514 nm, λ_{em} = 595 nm) at 25 °C. 100 µL of solution A were used for the Sp1-f3, and 50 µL of solution A were used for the AMPB-Sp1-f3. Fluorescence emission was plotted against the [EB]/[peptide] ratio. The data were fitted with exponential decay first order curve, which provides the IC_{50} value representing the ratio [EB]/[peptide] necessary to displace half of the molecules of ethidium bromide in the complex EB/DNA.[25]

6.6 References

[1] a) A. A. Beharry, G. A. Woolley, *Chem. Soc. Rev.,* 2011, **40**, 4422. b) W. Szymański, J. M. Beierle, H. A. V. Kistemaker, W. A. Velema, B. L. Feringa, *Chem. Rev.*, 2013, **113**, 6114. c) C. Renner, L. Moroder, *Chem. Bio. Chem.*, 2006, **7**, 869. d) F. Ciardelli, S. Bronco, P. Pieroni, A. Pucci, in Photo-switchable Polypeptides. B. L. Feringa, W. R. Browne, Eds.; Molecular Switches, 2nd ed.; Wiley-VCH: Weinheim, 2011; Chapter 10.

[2] a) R. Siewertsen, H. Neumann, B. Buchheim-Stehn, R. Herges, C. Naether, F. Renth, F. Temps, *J. Am. Chem. Soc*., 2009, **131**, 15594. b) A. A. Beharry, O. Sadovski, G. A. Woolley, *J. Am. Chem. Soc*. 2011, **133**, 19684. c) W. A. Velema, W. Szymanski, B. L. Feringa, *J. Am. Chem. Soc*., 2014, **136**, 2178.

[3] a) D. Brash, J. Rudolph, J. Simon, A. Lin, G. Mckenna, H. Baden, A. Halperin, J. Ponten, *Proc. Natl. Acad. Sci. U.S.A.* 1991, **88**, 10124. b) M. Protic-Sabljic, N. Tuteja, P. Munson, J. Hauser, K. Kraemer, K. Dixon, *Mol. Cell. Biol.,* 1986, **6**, 3349.

[4] a) D. H. Waldeck, *Chem. Rev.* 1991, **91**, 415. b) W. G. Han, T. Lovell, T. Q. Liu, L. Noodleman, *ChemPhysChem*, 2002, **3**, 167.

[5] a) V. I. Minkin, In Photoswitchable Molecular Systems Based on Spiropyrans and Spirooxazines, Feringa, B. L.; Browne, W. R., Eds.; Molecular Switches, 2nd ed.; Wiley-VCH: Weinheim, 2011; Chapter 2.

[6] a) M. Irie, *Chem. Rev*. 2000, **100**, 1685. b) C. C. Warford, V. Lemieux, N. R. Branda, N. R. Multifunctional Diarylethenes. Feringa, B. L.; Browne, W. R., Eds.; Molecular Switches, 2nd ed.; Wiley-VCH: Weinheim, 2011; Chapter 1.

[7] a) H. M. Bandara, S. C. Burdette, *Chem. Soc. Rev.*, 2012, **41**, 1809. b) F. Hamon, F. Djedaini-Pilard, F. Barbot, C. Len, *Tetrahedron*, 2010, **66**, 2538. c) F. Hamon, F. Djedaini-Pilard, F. Barbot, C. Len, *Tetrahedron* 2009, **65**, 10105. d) N. Nishimura, T. Sueyoshi, H. Yamanaka, E. Imai, S. Yamamoto, S. Hasegawa, *Bull. Chem. Soc. Jpn.*, 1976, **49**, 1381. e) P. Bortolus, S. Monti, *J. Phys. Chem*. 1979, **83**, 648.

[8] For recent examples on photocontrolling the α-helix, see: a) A. A. Beharry, G. A. Woolley, *Neuromethods*, 2011, **55**, 171. b) G. Merutka, W. Shalongo, E. Stellwagen, *Biochemistry*, 1991, **30**, 4245. c) D. C. Burns, F. Zhang, G. A. Woolley, *Nat. Protocols*, 2007, **2**, 251. d) A. A. Ali, G. A. Woolley, *Org. Biomol. Chem.*, 2013, **11**, 5325. e) M. Blanco-Lomas, S. Samanta, P. J. Campos, G. A. Woolley, *J. Am. Chem. Soc*., 2012, **134**, 6960. f) S. Samanta, C. Qin, A. J. Lough, G. A. Woolley, *Angew. Chem. Int. Ed*., 2012, **51**, 6452. g) S. Samanta, A. A. Beharry, O. Sadovski, T. M. McCormick, A. Babalhavaeji, V. Tropepe, G. A. Woolley, *J. Am. Chem. Soc*., 2013, **135**, 9777. h)

L. Nevola, A. Martín-Quirós, K. Eckelt, N. Camarero, S. Tosi, A. Llobet, E. Giralt, P. Gorostiza, *Angew. Chem. Int. Ed*., 2013, **52**, 7704.

[9] For recent examples on photocontrolling the leucine zipper domains, see: a) J. R. Kumita, D. G., Flint, G. A., Woolley, O. S. Smart, *Faraday Discuss.*, 2003, **122**, 89. b) A. M. Caamaño, M. E. Vaźquez, J. Martínez-Costas, L. Castedo, J. L. Mascareñas, *Angew. Chem., Int. Ed.,* 2000, **39**, 3104. c) G. A. Woolley, A. S. I. Jaikaran, M. Berezovski, M.; J. P. Calarco, S. N. Krylov, O. S. Smart, J. R. Kumita, *Biochemistry*, 2006, **45**, 6075.

[10] J. R. Kumita, O. S. Smart, G. A. Woolley, *Proc. Natl. Acad. Sci. U. S. A.*, 2000, **97**, 3803.

[11] For recent examples on photocontrolling the β-hairpin structures, see: a) S.-L. Dong, M. Lçweneck, T. E. Schrader, W. J. Schreier, W. Zinth, L. Moroder, C. Renner, *Chem. Eur. J.,* 2006, **12**, 1114. b) A. Aemissegger, V. Kräutler, W. F. van Gunsteren, D. Hilvert, *J. Am. Chem. Soc.,* 2005, **127**, 2929. c) A. A. Deeg, M. S. Rampp, A. Popp, B. M. Pilles, T. E. Schrader, L. Moroder, K. Hauser, W. Zinth, *Chem. Eur. J.*, 2014, **20**, 694. d) T. Podewin, M. S. Rampp, I. Turkanovic, K. L. Karaghiosoff, W. Zinth, A. Hoffmann-Röder, *Chem. Commun.*, 2015, 4001.

[12] a) A. Klug, *Annu. Rev. Biochem.*, 2010, **79**, 213. b) S. A. Wolfe, L. Nekludova, C. O. Pabo, *Annu. Rev. Biophys. Biomol. Struct*., 1999, **3**, 183.

[13] J. Miller, A.D. McLachlan, A. Klug, *The EMBO Journal*, 1985, **4**, 1609.

[14] C. Chou, A. Deiters, *Angew. Chem. Int. Ed.,* 2011, **50**, 6839.

[15] A. Nomura, A. Okamoto, *Chem. Commun.,* 2009, 1906.

[16] a) R. Behrendt, M. Schenk, H.-J. Musiol, L. Moroder, *J. Peptide Sci.*, 1999, **5**, 519. b) L. Ulysse, J. Chmielewski, *Bioorg. Med. Chem. Lett.,* 1994, **4**, 2145.

[17] a) V. A. Narayan, R. W. Kriwacki, J. P. Caradonna, *J. Biol. Chem.,* 1997, **272**, 7801. b) M. Yokono, N. Saegusa, K. Matsushita, Y. Sugiura, *Biochemistry*, 1998, **37**, 6824. c) S. Oka, Y. Shiraishi, T. Yoshida, T. Ohkubo, Y. Sugiura, Y. Kobayashi, *Biochemistry*, 2004, **43**, 16027.

[18] B. Priewisch, K. Rück-Braun, *J. Org. Chem.,* 2005, **70**, 2350.

[19] M. Löweneck, A. G. Milbradt, C. Root, H. Satzger, W. Zinth, L. Moroder, and C. Renner, *Biophys. J.*, 2006, **90**, 2099.

[20] The photostationary state measured by HPLC is underrepresentative for the real value due to the thermal *cis-trans* isomerisation during the analysis.

[21] A. D. Frankel, J. M. Berg, C. O. Pabo, *Proc. Natl. Acad. Sci. USA,* 1987, **84**, 4841.

[22] Y.-H. Shim, P. B. Armondo, A. Laigle, A. Garbesi, S. Lavielle, *Org. Biomol. Chem*., 2004, **2**, 915.

[23] H. Y. Kuchelmeister, S. Karczewski, A. Gutschmidt, S. Knauer, C. Schmuck, *Angew. Chem. Int. Ed.,* 2013, **52**, 14016.

[24] F. Tibiletti, M. Simonetti, K. M. Nicholas, G. Palmisano, M. Parravicini, F. Imbesi, S. Tollari, A. Penoni, *Tetrahedron*, 2010, **66**, 1280.

[25] H. Y. Kuchelmeister, S. Karczewski, A. Gutschmidt, S. Knauer, C. Schmuck, *Angew. Chem. Int. Ed.*, 2013, **52**, 14016.